Journal of Thermal Stresses
Publication details, including instructions for authors and subscription information:
http://www.informaworld.com/smpp/title~content=t713723680

Thermo-Mechanical Analysis Of Functionally Graded Shells

M. Cinefra[a]; E. Carrera[b]; S. Brischetto[b]; S. Belouettar[a]
[a] Centre de Recherche Public Henri Tudor, Luxembourg [b] Department of Aeronautics and Space Engineering, Politecnico di Torino, Italy

Online publication date: 04 October 2010

To cite this Article Cinefra, M. , Carrera, E. , Brischetto, S. and Belouettar, S.(2010) 'Thermo-Mechanical Analysis Of Functionally Graded Shells', Journal of Thermal Stresses, 33: 10, 942 — 963
To link to this Article: DOI: 10.1080/01495739.2010.482379
URL: http://dx.doi.org/10.1080/01495739.2010.482379

Journal of Thermal Stresses, 33: 942–963, 2010

ISSN: 0149-5739 print/1521-074X online
DOI: 10.1080/01495739.2010.482379

Taylor & Francis
Taylor & Francis Group

THERMO-MECHANICAL ANALYSIS OF FUNCTIONALLY GRADED SHELLS

M. Cinefra[1], E. Carrera[2], S. Brischetto[2], and S. Belouettar[1]
[1]*Centre de Recherche Public Henri Tudor, Luxembourg*
[2]*Department of Aeronautics and Space Engineering, Politecnico di Torino, Italy*

The thermo-mechanical analysis of a simply supported, functionally graded shell is considered in this work. Refined shell theories are considered to account for grading material variation in the thickness direction. The governing thermodynamical equations are derived from the Principle of Virtual Displacements. The distribution of the temperature field $T(z)$ is not assumed linear in the thickness direction of the layered shells and Fourier's heat conduction equation is solved to provide $T(z)$. Classical and higher order shell theories are implemented in cases of both an equivalent single layer and layer-wise variable description by referring to Carrera's Unified Formulation. The numerical results show temperature, displacement and stress distributions along the thickness direction. Different volume fractions of the metallic and ceramic constituents as well as different shell thickness ratios and orders of expansion are analyzed. These are in good agreement with the quasi-3D solution obtained considering mathematical layers with constant properties in the FGM layer and using high orders of expansion.

Keywords: Carrera unified formulation; Functionally graded materials; Heat conduction; Refined theories; Shell theories; Thermal stress

INTRODUCTION

The concept of *Functionally Graded Materials* (FGMs) was first proposed in Japan in the late 1980s, as a thermal barrier material [1, 2]. The severe temperature loads involved in many engineering applications, such as thermal barrier coatings, engine components or rocket nozzles, require materials that are resistant to high temperatures. FGMs are advanced composite materials in which the composition of each material constituent varies gradually with respect to the spatial coordinates. Therefore, the macroscopic material properties in FGMs vary continuously, thus distinguishing them from laminated composite materials in which the abrupt change in material properties across layer interfaces leads to large interlaminar stresses, which allow damage to develop. As in the case of laminated composite materials, FGMs combine the desirable properties of the constituent phases to obtain a superior performance and avoid the problem of interfacial stresses.

Communicated by Pier Marzocca on 13 December 2009.
Authors acknowledge the partial support of Piemonte Regional Project STEPS. M. Cinefra acknowledges the support of FNR of Luxembourg.
Address correspondence to M. Cinefra, Department of Aeronautics and Space Engineering, Politecnico di Torino, Corso Duca degli Abruzzi, 24, Torino 10129, Italy. E-mail: maria.cinefra@polito.it

In the field of FGMs, three problems are substantially dealt with, namely: development of processing routes for functionally graded materials [3–6], determination of the spatially varying material properties (material modeling) [7–10] and modeling of structures comprising FGMs. The present work is focused on the latter topic.

Over the last decade, extensive research has been carried out on the modeling of shells comprising FGM layers. Pelletier and Vel [11] have provided an exact solution for the steady-state thermoelastic response of functionally graded orthotropic cylindrical shells. The equilibrium equations are solved by the power series method and the temperature field are obtained by solving the heat conduction equations. The cylindrical shells are analyzed using the Flugge and the Donnell shell theories. Shao [12] has derived a series solution for a mullite/molybdenum functionally graded circular hollow cylinder, using a multi-layered approach based on the laminated composite theory. The material properties are assumed to be temperature-independent and radial dependent, but are assumed to be homogenous in each layer. The temperature profile along the thickness is calculated by means of the heat conduction equations. A functionally graded circular hollow cylinder has also been analyzed by Liew et al. [13]. In this case, the solutions are obtained through a novel limiting process that employs the solutions of homogeneous hollow circular cylinders, without making recourse to the basic theory or the non-homogeneous thermoelasticity equations. The temperature distribution is assumed in the radial direction. They conclude that thermal stresses necessarily occur in the FGM cylinder and that heat resistance may be improved by sagaciously designing the material composition.

Vel and Baskiyar [14] have presented an analytical solution for a two-constituent isotropic metal/ceramic functionally graded tube with arbitrary variation of the material properties in the radial direction and subjected to steady thermomechanical loads. The heat conduction and thermoelasticity equations are solved using the power series method to obtain the temperature, displacements and thermal stresses. Abrinia et al. [15] have proposed an analytical method to compute the radial and circumferential stresses in a thick FGM cylindrical vessel under the influence of internal pressure and temperature. In this paper it is assumed that the modulus of elasticity and thermal coefficient of expansion vary through the thickness of the FGM material, according to a power law relationship. The effect of non-homogeneity in the FGM cylinder is implemented by choosing a dimensionless parameter β, which could be assigned an arbitrary value that could affect the stresses in the cylinder. Shao and Wang [16] have performed a three-dimensional thermoelastic analysis of a functionally graded cylindrical panel with finite length and subjected to nonuniform mechanical and steady-state thermal loads.

The thermal and mechanical properties are assumed to be temperature independent and continuously vary in the radial direction of the panel. Analytical solutions for the temperature and stress fields are expressed in terms of trigonometric and power series that are only suitable for the simply supported boundary conditions. Some researchers have instead treated the same problem with finite element approaches. In [17], mixed-interpolated finite elements have been used to study cylindrical shells made of functionally graded materials. A two-constituent material distribution through the thickness is assumed to vary with a simple mixture

power rule. The governing equations are determined using a variational formulation that arises from the Naghdi theory.

A strategy to evaluate an improved shear corrector factor has been adopted, taking into account the variation in the shear stress through the shell thickness. Naghdabadi and Kordkheili [18] have proposed a finite element formulation for the thermoelastic analysis of functionally graded plates and shells. The power law distribution model has been assumed for the composition of the constituent materials in the thickness direction. The procedure adopted to derive the finite element formulation inherently contains the analytical through-the-thickness integration, without using the Gauss points. This integration is become possible due to the proper decomposition of the material properties into the product of a scalar variable and a constant matrix through the thickness. They then took into account the geometrically non-linear thermoelastic behavior of FGM plates and shells in [19], where the finite element formulation is derived using the updated Lagrangian approach and it is based on a rewriting of the Green-Lagrange strain as well as the 2nd Piola-Kirchoff stress as two second-order functions, in terms of a through-the-thickness parameter. This makes it possible to account for the non-linearities in the material properties and temperature distribution in the thickness direction. In both cases, the nonlinear heat transfer equation is solved for thermal distribution using the Rayleigh-Ritz method. In literature, it is possible to find other works about the thermo-mechanical problem in functionally graded shells, such as [20], in which the coupled thermoelastic response of an FGM shell is studied or [21], where thermo-mechanical properties of FGM are assumed to be temperature-dependent, but they are not part of our field of interest.

In the present work, the Carrera Unified Formulation (CUF), which was developed by Carrera for multi-layered structures [22] is extended to also account for functionally graded shells under mechanical and thermal loadings. In [23, 24], the Principle of Virtual Displacements (PVD) has been proposed and the extension to Reissner's Mixed Variational Theorem (RMVT) has been given in [25]. The thermo-mechanical bending problem of functionally graded plates has already been proposed in [26]. This paper addresses the static response of functionally graded shells and the governing equations are derived from the Principle of Virtual Displacements, considering the temperature as an external load only. The thermo-mechanical properties of FGM are assumed to be temperature independent. The solution procedures have been implemented in the in-house code MUL2 [27].

UNIFIED FORMULATION

In case of bi-dimensional multi-layered structures (plates and shells), Unified Formulation by Carrera [22] permits to obtain a large variety of 2D models that differ in the order of used expansion in thickness direction and in the manner the variables are modelled (Equivalent Single Layer (ESL) or Layer Wise (LW) approach). The salient feature of Unified Formulation is the unified manner in which all considered variables and fields (displacement, temperature, material) can be treated. As usual in shell theories, the considered variables and their variation are splitted in a set of thickness functions and the relative terms only depending on

in-plane coordinates (α, β). According to this separation, a general variable $\boldsymbol{a}$ and its respective variation $\delta\boldsymbol{a}$ can be written as:

$$\boldsymbol{a}(\alpha, \beta, z) = F_\tau(z)\boldsymbol{a}_\tau(\alpha, \beta) \quad \delta\boldsymbol{a}(\alpha, \beta, z) = F_s(z)\delta\boldsymbol{a}_s(\alpha, \beta) \quad \text{with } \tau, s = 1, \ldots, N \tag{1}$$

where N is the order of expansion in the thickness direction.

Due to the unified treatment of all variables, the three displacement components u_α, u_β and u_z and their relative variations can be modelled via Unified Formulation, irrespective of whether FGM layers or constant property layers (also indicated here as classical layers) are considered. A typical single layer FGM structure is reported in Figure 1. In case of Equivalent Single Layer (ESL) models, the expansion of the displacement components is assumed for the whole multi-layer:

$$(u_\alpha, u_\beta, u_z) = F_\tau(u_{\alpha\tau}, u_{\beta\tau}, u_{z\tau}) \quad (\delta u_\alpha, \delta u_\beta, \delta u_z) = F_s(\delta u_{\alpha s}, \delta u_{\beta s}, \delta u_{zs}) \tag{2}$$

with Taylor expansions from first up to 14th orders: $F_0 = z^0 = 1$, $F_1 = z^1 = z, \ldots, F_N = z^N, \ldots, F_{14} = z^{14}$.

In case of Layer Wise (LW) models, each layer k of the given multi-layered structure is separately considered:

$$(u_\alpha^k, u_\beta^k, u_z^k) = F_\tau^k(u_{\alpha\tau}^k, u_{\beta\tau}^k, u_{z\tau}^k) \quad (\delta u_\alpha^k, \delta u_\beta^k, \delta u_z^k) = F_s^k(\delta u_{\alpha s}^k, \delta u_{\beta s}^k, \delta u_{zs}^k) \tag{3}$$

where combinations of Legendre polynomials are employed as thickness functions:

$$F_t = \frac{P_0 + P_1}{2} \quad F_b = \frac{P_0 - P_1}{2} \quad F_l = P_l - P_{l-2} \quad \text{with } \tau, s = t, b, l \text{ and } l = 2, \ldots, 14 \tag{4}$$

Here, t and b indicate the top and bottom values for each layer, P_l are the Legendre polynomials ($P_0 = 1$, $P_1 = \zeta_k$, $P_2 = \frac{(3\zeta_k^2 - 1)}{2}$ and so on) with $\zeta_k = \frac{2z^k}{h^k}$ that is the non-dimensionalized thickness coordinate ranging from -1 to $+1$ in each layer k. z_k is the local coordinate and h_k is the thickness of the kth layer.

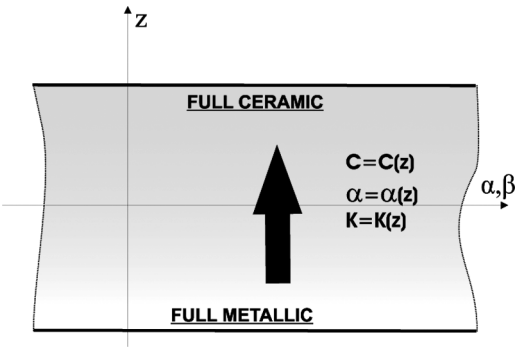

Figure 1 Example of a single-layered FGM structure.

The chosen functions have the following interesting properties:

$$\begin{aligned} &\zeta_k = +1: \quad F_t = 1; \quad F_b = 0; \quad F_l = 0 \quad \text{at the top} \\ &\zeta_k = -1: \quad F_t = 0; \quad F_b = 1; \quad F_l = 0 \quad \text{at the bottom} \end{aligned} \tag{5}$$

It is obvious that for a single layer shell the ESL and LW evaluations coincide. For further details about UF for multi-layered structures and the relative assembling procedure of stiffness matrix the reader can refer to [22, 28, 29].

Unified Formulation for Temperature Profile

In the present model the temperature is seen as an external load. If the values of the temperature are known at the top and bottom surface of the plate, the thermal load can be considered in two different ways. The first method introduces an assumed profile $T(z)$ that varies linearly from the top to the bottom; the second one computes $T(z)$ by solving Fourier's heat conduction equation [30]. In this paper only the second way is considered, because even for a very thin FGM layer the temperature profile is nonlinear. Therefore, the assumption of a linear $T(z)$ would cause very large errors.

The temperature profile is described in the same way as the displacements in case of the Layer Wise approach:

$$T^k(\alpha, \beta, z) = F_\tau \theta_\tau^k \quad \text{with } \tau = t, b, l \text{ and } l = 2, \ldots, 14 \tag{6}$$

Again, t and b indicate top and the bottom of the considered kth layer. The thickness functions F_τ are a combination of Legendre polynomials.

If the considered shell is subjected to a bi-sinusoidal temperature at the top and the bottom, the thermal boundary conditions are:

$$\begin{aligned} &T = 0 \quad \text{at } \alpha = 0, a \text{ and } \beta = 0, b \\ &T = T_b \sin\left(\frac{m\pi\alpha}{a}\right) \sin\left(\frac{n\pi\beta}{b}\right) \quad \text{at } z = -\frac{h}{2} \text{ with } b: \text{bottom} \\ &T = T_t \sin\left(\frac{m\pi\alpha}{a}\right) \sin\left(\frac{n\pi\beta}{b}\right) \quad \text{at } z = +\frac{h}{2} \text{ with } t: \text{top} \end{aligned} \tag{7}$$

where m and n are the waves number along the two in-plane shell directions (α, β). a and b are the shell dimensions, h is the shell thickness, and T_b and T_t are the amplitudes of the temperature at the bottom and the top, respectively.

In general for the kth homogeneous orthotropic layer, the differential Fourier's equation of heat conduction reads:

$$\left(\frac{K_1^k}{H_\alpha^2}\right)\frac{\partial^2 T}{\partial \alpha^2} + \left(\frac{K_2^k}{H_\beta^2}\right)\frac{\partial^2 T}{\partial \beta^2} + K_3^k \frac{\partial^2 T}{\partial z^2} = 0 \tag{8}$$

K_1^k, K_2^k and K_3^k are the thermal conductivities along the three shell directions α, β and z; they are constant in each layer in case of classical materials, but they depend

by the thickness coordinate in case of FGMs. ∂ indicates the partial derivative. $H_\alpha = (1 + z^k/R_\alpha^k)$ and $H_\beta = (1 + z^k/R_\beta^k)$ are the metric coefficients. In case of plates the Eq. (8) has $H_\alpha = H_\beta = 1$ and the coefficients K_1^k, K_2^k and K_3^k depend on z because some layers k can be in FGM. In case of shell we can define three new coefficients $K_1^{*k} = \frac{K_1^k(z)}{H_\alpha^2}$, $K_2^{*k} = \frac{K_2^k(z)}{H_\beta^2}$ and $K_3^{*k} = K_3^k(z)$, which in a generic layer k depend on the thickness coordinate of the shell. K_1^{*k} and K_2^{*k} can depend by the thickness coordinate z for two reasons: possible use of FGM layers and/or presence of curvature in case of shells; K_3^{*k} can depend by z coordinate only in case of FGM layers. So Fourier's equation becomes:

$$K_1^{*k}\frac{\partial^2 T}{\partial \alpha^2} + K_2^{*k}\frac{\partial^2 T}{\partial \beta^2} + K_3^{*k}\frac{\partial^2 T}{\partial z^2} = 0 \tag{9}$$

Equation (9) has not constant coefficients in the layer k. It can be solved by introducing, for each layer k, a given number of mathematical layers (N_{ml}) in which K_1^{*k}, K_2^{*k} and K_3^{*k} can be supposed constant. In each mathematical layer, the values of H_α and H_β and the material properties of the FGM layer can be calculated at a given value of the coordinate z, so the mean value between the values at the top and bottom of mathematical layer is taken for K_1^j, K_2^j and K_3^j, while the value at the midsurface is taken for H_α and H_β. The complete procedure to calculate the actual temperature profile $T_c(z)$ and to obtain the values of θ_τ^k for Eq. (6) is reported in [26], where the plate case is considered, but the Fourier's equation is formally the same ($K_1^{*k} = K_1^k$, $K_2^{*k} = K_2^k$ and $K_3^{*k} = K_3^k$ for the plate).

GOVERNING EQUATIONS

This section presents the derivation of the governing equations based on the *Principle of Virtual Displacements* (PVD) in case of an FGM shell subjected to thermal and/or external mechanical loads. A closed form solution will be developed considering particular material and boundary conditions. The procedure permits to obtain the so-called *fundamental nuclei* that are simple matrices representing the basic element from which the stiffness matrix of the whole structure can be computed.

A multi-layered shell with N_l layers, some of which could be FGM layers, is considered. The PVD for the thermo-mechanical case reads:

$$\sum_{k=1}^{N_l}\int_{\Omega_k}\int_{A_k}\left\{\delta\boldsymbol{\epsilon}_{pG}^{k\,T}\boldsymbol{\sigma}_{pC}^k + \delta\boldsymbol{\epsilon}_{nG}^{k\,T}\boldsymbol{\sigma}_{nC}^k\right\}d\Omega_k dz = \sum_{k=1}^{N_l}\delta L_e^k \tag{10}$$

where Ω_k and A_k are the integration domains in plane (α, β) and z direction, respectively. k indicates the layer and T the transpose of a vector. δL_e^k is the external work for the kth layer. G means geometrical relations and C constitutive equations. $\boldsymbol{\sigma}_{pC}$ and $\boldsymbol{\sigma}_{nC}$ contain the mechanical (d) and thermal (t) contributions, so:

$$\sum_{k=1}^{N_l}\int_{\Omega_k}\int_{A_k}\left\{\delta\boldsymbol{\epsilon}_{pG}^{k\,T}(\boldsymbol{\sigma}_{pd}^k - \boldsymbol{\sigma}_{pt}^k) + \delta\boldsymbol{\epsilon}_{nG}^{k\,T}(\boldsymbol{\sigma}_{nd}^k - \boldsymbol{\sigma}_{nt}^k)\right\}d\Omega_k dz = \sum_{k=1}^{N_l}\delta L_e^k \tag{11}$$

The steps to obtain the governing equations are:

- Substitution of the geometrical relations (subscript G)
- Substitution of the appropriate constitutive equations (subscript C)
- Introduction of the Unified Formulation

Geometrical Relations

The shells are bi-dimensional structures in which one dimension (in general the thickness in z direction) is negligible with respect to the other two in-plane dimensions. Geometry and the reference system are indicated in Figure 2. The square of an infinitesimal linear segment in the layer, the associated infinitesimal area and the volume are given by:

$$\begin{aligned} ds_k^2 &= H_\alpha^{k^2} d\alpha_k^2 + H_\beta^{k^2} d\beta_k^2 + H_z^{k^2} dz_k^2 \\ d\Omega_k &= H_\alpha^k H_\beta^k d\alpha_k d\beta_k \\ dV &= H_\alpha^k H_\beta^k H_z^k d\alpha_k d\beta_k dz_k \end{aligned} \tag{12}$$

where the metric coefficients are:

$$H_\alpha^k = A^k(1 + z_k/R_\alpha^k), \quad H_\beta^k = B^k(1 + z_k/R_\beta^k), \quad H_z^k = 1 \tag{13}$$

k denotes the k-layer of the multilayered shell; R_α^k and R_β^k are the principal radii of curvature along the coordinates α_k and β_k, respectively. A^k and B^k are the coefficients of the first fundamental form of Ω_k (Γ_k is the Ω_k boundary). In this paper, the attention has been restricted to the shells with constant radii of curvature (cylindrical, spherical, toroidal geometries) for which $A^k = B^k = 1$. The details for the shells are reported in [31].

From this point on, stresses and strains are going to be separated into in-plane and normal components, denoted respectively by the subscripts p and n.

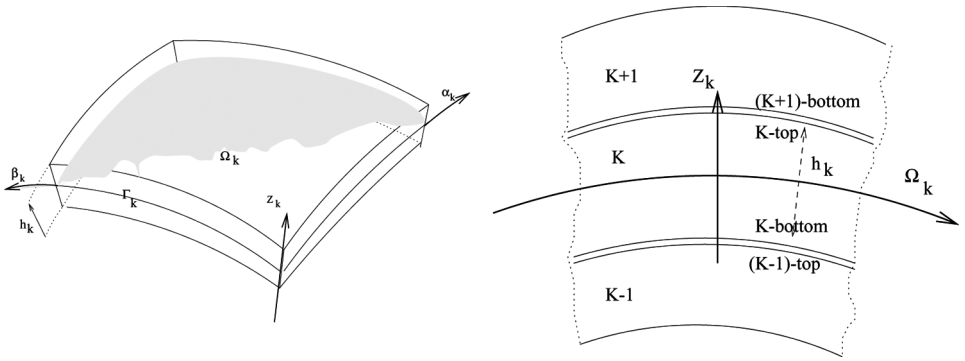

Figure 2 Geometry and notations for a multilayered shell (doubly curved).

The mechanical strains in the kth layer can be related to the displacement field $\boldsymbol{u}^k = \{u_\alpha^k, u_\beta^k, u_z^k\}$ via the geometrical relations:

$$\begin{aligned}\boldsymbol{\epsilon}_{pG}^k &= [\epsilon_{\alpha\alpha}, \epsilon_{\beta\beta}, \gamma_{\alpha\beta}]^{kT} = (\boldsymbol{D}_p^k + \boldsymbol{A}_p^k)\boldsymbol{u}^k \\ \boldsymbol{\epsilon}_{nG}^k &= [\gamma_{\alpha z}, \gamma_{\beta z}, \epsilon_{zz}]^{kT} = (\boldsymbol{D}_{np}^k + \boldsymbol{D}_{nz}^k - \boldsymbol{A}_n^k)\boldsymbol{u}^k\end{aligned} \tag{14}$$

wherein the differential operator arrays are defined as follows:

$$\boldsymbol{D}_p^k = \begin{bmatrix} \frac{\partial_\alpha}{H_\alpha^k} & 0 & 0 \\ 0 & \frac{\partial_\beta}{H_\beta^k} & 0 \\ \frac{\partial_\beta}{H_\beta^k} & \frac{\partial_\alpha}{H_\alpha^k} & 0 \end{bmatrix}, \quad \boldsymbol{D}_{np}^k = \begin{bmatrix} 0 & 0 & \frac{\partial_\alpha}{H_\alpha^k} \\ 0 & 0 & \frac{\partial_\beta}{H_\beta^k} \\ 0 & 0 & 0 \end{bmatrix}, \quad \boldsymbol{D}_{nz}^k = \begin{bmatrix} \partial_z & 0 & 0 \\ 0 & \partial_z & 0 \\ 0 & 0 & \partial_z \end{bmatrix} \tag{15}$$

$$\boldsymbol{A}_p^k = \begin{bmatrix} 0 & 0 & \frac{1}{H_\alpha^k R_\alpha^k} \\ 0 & 0 & \frac{1}{H_\beta^k R_\beta^k} \\ 0 & 0 & 0 \end{bmatrix}, \quad \boldsymbol{A}_n^k = \begin{bmatrix} \frac{1}{H_\alpha^k R_\alpha^k} & 0 & 0 \\ 0 & \frac{1}{H_\beta^k R_\beta^k} & 0 \\ 0 & 0 & 0 \end{bmatrix} \tag{16}$$

Here, $\boldsymbol{\epsilon}_p$ and $\boldsymbol{\epsilon}_n$ contain both the mechanical and thermal contributes.

Constitutive Equations

In case of thermo-mechanical problems, the constitutive equations are given as:

$$\begin{aligned}\boldsymbol{\sigma}_{pC}^k &= \boldsymbol{\sigma}_{pd}^k - \boldsymbol{\sigma}_{pt}^k = \boldsymbol{C}_{pp}^k(z)\boldsymbol{\epsilon}_{pG}^k + \boldsymbol{C}_{pn}^k(z)\boldsymbol{\epsilon}_{nG}^k - \boldsymbol{\lambda}_p^k(z)T^k \\ \boldsymbol{\sigma}_{nC}^k &= \boldsymbol{\sigma}_{nd}^k - \boldsymbol{\sigma}_{nt}^k = \boldsymbol{C}_{np}^k(z)\boldsymbol{\epsilon}_{pG}^k + \boldsymbol{C}_{nn}^k(z)\boldsymbol{\epsilon}_{nG}^k - \boldsymbol{\lambda}_n^k(z)T^k\end{aligned} \tag{17}$$

where the coefficients $\boldsymbol{\lambda}_p^k(z)$ and $\boldsymbol{\lambda}_n^k(z)$ are linked to the coefficients of thermal expansion $\boldsymbol{\alpha}_p^k(z)$ and $\boldsymbol{\alpha}_n^k(z)$ by:

$$\begin{aligned}\boldsymbol{\lambda}_p^k(z) &= \boldsymbol{\lambda}_{pp}^k(z) + \boldsymbol{\lambda}_{pn}^k(z) = \boldsymbol{C}_{pp}^k(z)\boldsymbol{\alpha}_p^k(z) + \boldsymbol{C}_{pn}^k(z)\boldsymbol{\alpha}_n^k(z) \\ \boldsymbol{\lambda}_n^k(z) &= \boldsymbol{\lambda}_{np}^k(z) + \boldsymbol{\lambda}_{nn}^k(z) = \boldsymbol{C}_{np}^k(z)\boldsymbol{\alpha}_p^k(z) + \boldsymbol{C}_{nn}^k(z)\boldsymbol{\alpha}_n^k(z)\end{aligned} \tag{18}$$

with

$$\begin{aligned}\boldsymbol{C}_{pp}^k(z) &= \begin{bmatrix} C_{11}(z) & C_{12}(z) & C_{16}(z) \\ C_{12}(z) & C_{22}(z) & C_{26}(z) \\ C_{16}(z) & C_{26}(z) & C_{66}(z) \end{bmatrix} \quad \boldsymbol{C}_{pn}^k(z) = \begin{bmatrix} 0 & 0 & C_{13}(z) \\ 0 & 0 & C_{23}(z) \\ 0 & 0 & C_{36}(z) \end{bmatrix} \\ \boldsymbol{C}_{np}^k(z) &= \begin{bmatrix} 0 & 0 & 0 \\ 0 & 0 & 0 \\ C_{13}(z) & C_{23}(z) & C_{36}(z) \end{bmatrix} \quad \boldsymbol{C}_{nn}^k(z) = \begin{bmatrix} C_{55}(z) & C_{45}(z) & 0 \\ C_{45}(z) & C_{44}(z) & 0 \\ 0 & 0 & C_{33}(z) \end{bmatrix}\end{aligned} \tag{19}$$

The thermal expansion coefficients and the coefficients of thermo-mechanical coupling are:

$$\boldsymbol{\alpha}_p^k(z) = \begin{bmatrix} \alpha_1(z) \\ \alpha_2(z) \\ \alpha_6(z) \end{bmatrix} \quad \boldsymbol{\alpha}_n^k(z) = \begin{bmatrix} 0 \\ 0 \\ \alpha_3(z) \end{bmatrix} \quad \boldsymbol{\lambda}_p^k(z) = \begin{bmatrix} \lambda_1(z) \\ \lambda_2(z) \\ \lambda_6(z) \end{bmatrix} \quad \boldsymbol{\lambda}_n^k(z) = \begin{bmatrix} 0 \\ 0 \\ \lambda_3(z) \end{bmatrix} \tag{20}$$

Generally, the variation of the material properties in the thickness direction can be described multiplying a material constant by a function of z, i.e.,

$$\boldsymbol{C}(z) = \boldsymbol{C}_0 \cdot f(z) \tag{21}$$

$$\boldsymbol{K}(z) = \boldsymbol{K}_0 \cdot g(z) \tag{22}$$

$$\boldsymbol{\alpha}(z) = \boldsymbol{\alpha}_0 \cdot h(z) \tag{23}$$

$$\boldsymbol{\lambda}(z) = \boldsymbol{C}(z) \cdot \boldsymbol{\alpha}(z) = \boldsymbol{C}_0 \cdot \boldsymbol{\alpha}_0 \cdot m(z) \tag{24}$$

The procedure does not depend on the thickness laws $f(z)$, $g(z)$, $h(z)$ and $m(z)$. Thus, any possible material gradient can be accounted for. Now, applying the ideas behind UF, the following expansions are made:

$$(\boldsymbol{C}_{pp}^k(z), \boldsymbol{C}_{pn}^k(z), \boldsymbol{C}_{np}^k(z), \boldsymbol{C}_{nn}^k(z)) = F_r(z)(\boldsymbol{C}_{ppr}^k, \boldsymbol{C}_{pnr}^k, \boldsymbol{C}_{npr}^k, \boldsymbol{C}_{nnr}^k) \tag{25}$$

$$(\boldsymbol{\lambda}_p^k(z), \boldsymbol{\lambda}_n^k(z)) = F_r(z)(\boldsymbol{\lambda}_{pr}^k, \boldsymbol{\lambda}_{nr}^k) \tag{26}$$

with $r = 1, \ldots, 10$ and the thickness functions F_r are taken in the same manner as in the LW expansion. The procedure to calculate $\boldsymbol{C}_r$ and $\boldsymbol{\lambda}_r$ arrays is proposed in [26].

Therefore, in case of FGM shells, the constitutive equations Eqs. (17) read:

$$\begin{aligned} \boldsymbol{\sigma}_{pC}^k &= \boldsymbol{\sigma}_{pd}^k - \boldsymbol{\sigma}_{pt}^k = F_r \boldsymbol{C}_{ppr}^k \boldsymbol{\epsilon}_{pG}^k + F_r \boldsymbol{C}_{pnr}^k \boldsymbol{\epsilon}_{nG}^k - F_r \boldsymbol{\lambda}_{pr}^k T^k \\ \boldsymbol{\sigma}_{nC}^k &= \boldsymbol{\sigma}_{nd}^k - \boldsymbol{\sigma}_{nt}^k = F_r \boldsymbol{C}_{npr}^k \boldsymbol{\epsilon}_{pG}^k + F_r \boldsymbol{C}_{nnr}^k \boldsymbol{\epsilon}_{nG}^k - F_r \boldsymbol{\lambda}_{nr}^k T^k \end{aligned} \tag{27}$$

Differential Equilibrium Equations

Substituting the geometrical relations Eqs. (14) and the constitutive equations Eqs. (27) into the variational statement Eq. (10), for the kth layer one has:

$$\begin{aligned} \int_{\Omega_k} \int_{A_k} \Big[& ((\boldsymbol{D}_p^k + \boldsymbol{A}_p^k)\delta\boldsymbol{u}^k)^T (F_r \boldsymbol{C}_{ppr}^k (\boldsymbol{D}_p^k + \boldsymbol{A}_p^k)\boldsymbol{u}^k \\ & + F_r \boldsymbol{C}_{pnr}^k (\boldsymbol{D}_{n\Omega}^k + \boldsymbol{D}_{nz}^k - \boldsymbol{A}_n^k)\boldsymbol{u}^k - F_r \boldsymbol{\lambda}_{pr}^k T^k) \\ & + ((\boldsymbol{D}_{n\Omega}^k + \boldsymbol{D}_{nz}^k - \boldsymbol{A}_n^k)\delta\boldsymbol{u}^k)^T (F_r \boldsymbol{C}_{npr}^k (\boldsymbol{D}_p^k + \boldsymbol{A}_p^k)\, \boldsymbol{u}^k \\ & + F_r \boldsymbol{C}_{nnr}^k (\boldsymbol{D}_{n\Omega}^k + \boldsymbol{D}_{nz}^k - \boldsymbol{A}_n^k)\boldsymbol{u}^k - F_r \boldsymbol{\lambda}_{nr}^k T^k) \Big] d\Omega_k dz = \delta L_e^k \end{aligned} \tag{28}$$

Now, if the expansions of UF Eqs. (2), (3) and (6) are implemented, it is obtained that:

$$\int_{\Omega_k}\int_{A_k}\Big[((\boldsymbol{D}_p^k+\boldsymbol{A}_p^k)F_s\delta\boldsymbol{u}_s^k)^T(F_r\boldsymbol{C}_{ppr}^k(\boldsymbol{D}_p^k+\boldsymbol{A}_p^k)F_\tau\boldsymbol{u}_\tau^k + F_r\boldsymbol{C}_{pnr}^k(\boldsymbol{D}_{n\Omega}^k+\boldsymbol{D}_{nz}^k-\boldsymbol{A}_n^k)F_\tau\boldsymbol{u}_\tau^k - F_r\boldsymbol{\lambda}_{pr}^kF_\tau\theta_\tau^k) + ((\boldsymbol{D}_{n\Omega}^k+\boldsymbol{D}_{nz}^k-\boldsymbol{A}_n^k)F_s\delta\boldsymbol{u}_s^k)^T(F_r\boldsymbol{C}_{npr}^k(\boldsymbol{D}_p^k+\boldsymbol{A}_p^k)F_\tau\boldsymbol{u}_\tau^k + F_r\boldsymbol{C}_{nnr}^k(\boldsymbol{D}_{n\Omega}^k+\boldsymbol{D}_{nz}^k-\boldsymbol{A}_n^k)F_\tau\boldsymbol{u}_\tau^k - F_r\boldsymbol{\lambda}_{nr}^kF_\tau\theta_\tau^k)\Big]d\Omega_k dz=\delta L_e^k \tag{29}$$

After integration by parts, the governing differential equations on domain Ω_k and boundary conditions on edge Γ_k are achieved. Further details on the procedure of integration by parts are reported in [24]. The governing equations for a FGM multilayered shell subjected to thermal and mechanical loadings are:

$$\delta\boldsymbol{u}_s^{kT}:\boldsymbol{K}_{uu}^{k\tau sr}\boldsymbol{u}_\tau^k=\boldsymbol{K}_{u\theta}^{k\tau sr}\boldsymbol{\theta}_\tau^k+\boldsymbol{P}_{u\tau}^k \tag{30}$$

where $(\boldsymbol{K}_{u\theta}^{k\tau sr}\boldsymbol{\theta}_\tau^k)$ is the thermal load and $\boldsymbol{P}_{u\tau}^k$ is the external mechanical load. The fundamental nuclei $\boldsymbol{K}_{uu}^{k\tau sr}$ and $\boldsymbol{K}_{u\theta}^{k\tau sr}$ have to be assembled by expanding the indices as described in the following: in case of a FGM layer, an internal loop on index r accounts for the variation of the material properties, via τ and s the expansion in z for the variables is considered, and via k the assembling on the number of layers is accomplished.

The fundamental nuclei are:

$$\boldsymbol{K}_{uu}^{k\tau s}=\int_{A_k}\Big[\big(-\boldsymbol{D}_p^{ks}+\boldsymbol{A}_p^{ks}\big)^T\big(\boldsymbol{C}_{ppr}^k(\boldsymbol{D}_p^{k\tau}+\boldsymbol{A}_p^{k\tau})+\boldsymbol{C}_{pnr}^k(\boldsymbol{D}_{n\Omega}^{k\tau}+\boldsymbol{D}_{nz}^{k\tau}-\boldsymbol{A}_n^{k\tau})\big) + \big(-\boldsymbol{D}_{n\Omega}^{ks}+\boldsymbol{D}_{nz}^{ks}-\boldsymbol{A}_n^{ks}\big)^T\big(\boldsymbol{C}_{npr}^k(\boldsymbol{D}_p^{k\tau}+\boldsymbol{A}_p^{k\tau}) + \boldsymbol{C}_{nnr}^k(\boldsymbol{D}_{n\Omega}^{k\tau}+\boldsymbol{D}_{nz}^{k\tau}-\boldsymbol{A}_n^{k\tau})\big)\Big]F_rF_sF_\tau H_\alpha^kH_\beta^kdz, \tag{31}$$

$$\boldsymbol{K}_{u\theta}^{k\tau s}=\int_{A_k}\Big[\big(-\boldsymbol{D}_p^{ks}+\boldsymbol{A}_p^{ks}\big)^T\big(-\boldsymbol{\lambda}_{pr}^k\big)+\big(-\boldsymbol{D}_{n\Omega}^{ks} + \boldsymbol{D}_{nz}^{ks}-\boldsymbol{A}_n^{ks}\big)^T\big(-\boldsymbol{\lambda}_{nr}^k\big)\Big]F_rF_sF_\tau H_\alpha^kH_\beta^kdz \tag{32}$$

Closed Form Solutions

A Navier-type closed form solution of the quoted governing equations could be obtained upon substitution of the harmonic expressions for the displacements and temperature as well for shells constituted by layers made of orthotropic material.

The following harmonic assumptions can be made for the field variables:

$$u_{\alpha_\tau}^k=\sum_{m,n}(\widehat{U}_{\alpha_\tau}^k)\cos\left(\frac{m\pi\alpha_k}{a_k}\right)\sin\left(\frac{n\pi\beta_k}{b_k}\right)\quad k=1,N_l$$

$$
\begin{aligned}
u^k_{\beta_\tau} &= \sum_{m,n} (\widehat{U}^k_{\beta_\tau}) \sin\left(\frac{m\pi\alpha_k}{a_k}\right) \cos\left(\frac{n\pi\beta_k}{b_k}\right) \quad \tau = t, b, r \\
u^k_{z_\tau} &= \sum_{m,n} (\widehat{U}^k_{z_\tau}) \sin\left(\frac{m\pi\alpha_k}{a_k}\right) \sin\left(\frac{n\pi\beta_k}{b_k}\right) \quad r = 2, N \\
\theta^k_\tau &= \sum_{m,n} (\hat{\theta}^k_\tau) \sin\left(\frac{m\pi\alpha_k}{a_k}\right) \sin\left(\frac{n\pi\beta_k}{b_k}\right)
\end{aligned}
\tag{33}
$$

where $\widehat{U}^k_{\alpha_\tau}$, $\widehat{U}^k_{\beta_\tau}$, $\widehat{U}^k_{z_\xi}$ and $\hat{\theta}^k_\tau$ are the amplitudes, m and n the wave numbers, and a_k and b_k the plate dimensions.

The explicit forms of the fundamental nuclei $\boldsymbol{K}^{k\tau sr}_{uu}$ and $\boldsymbol{K}^{k\tau sr}_{u\theta}$ are given in Appendix A.

If $\theta^k_\tau = 0$ in Eq. (30), only a mechanical load is considered. Vice versa, if $\boldsymbol{P}^k_{u\tau} = 0$, only a thermal load is applied. If one considers a multi-layered structure comprising FGM and/or "classical" layers, two types of assembling procedures are possible: Equivalent Single Layer approach or Layer Wise approach. The fundamental nuclei are formally the same in case of "classical" or FGM layers; the only difference is the assembling loop on index r which accounts for the variation of the material properties through the thickness. In case of a single FGM layer, no multi-layer assembling procedure is necessary. Thus, in this case there is no difference between ESL and LW models. For more details about assembling procedure one can refers to [26].

Implemented Theories

A shell constituted by only one FGM layer is considered, along with two different loading conditions: pure mechanical and thermal loadings, both applied at the top of the shell. In case of only one layer, there is no difference among ESL or LW models. The used shell theory kinematics are therefore only denoted by the order N used for the description of the displacement $\boldsymbol{u}$ and the temperature T along the thickness direction ($N = 1, \ldots, 14$); the same order is used for these two variables. The proposed model is able also to describe multi-layered FGM/classical structures. These are not addressed in the present work.

RESULTS AND DISCUSSION

In this section a shell with geometry given by Ren, as shown in Figure 3, comprising a single functionally graded layer, is analyzed. As a typical example for high-temperature applications, the constituent materials of the functionally graded shell are taken to be Monel (70Ni-30Cu), a nickel-based alloy, and the ceramic zirconia (ZrO_2). The required material properties are those reported in [32]:

$$
\begin{aligned}
&B_m = 227.24\,\text{GPa}, \quad \mu_m = 65.55\,\text{GPa}, \quad \alpha_m = 15 \times 10^{-6}/\text{K}, \\
&K_m = 25\,\text{W/mK}, \quad \text{for Monel} \\
&B_c = 125.83\,\text{GPa}, \quad \mu_c = 58.08\,\text{GPa}, \quad \alpha_c = 10 \times 10^{-6}/\text{K}, \\
&K_c = 2.09\,\text{W/mK}, \quad \text{for zirconia}
\end{aligned}
$$

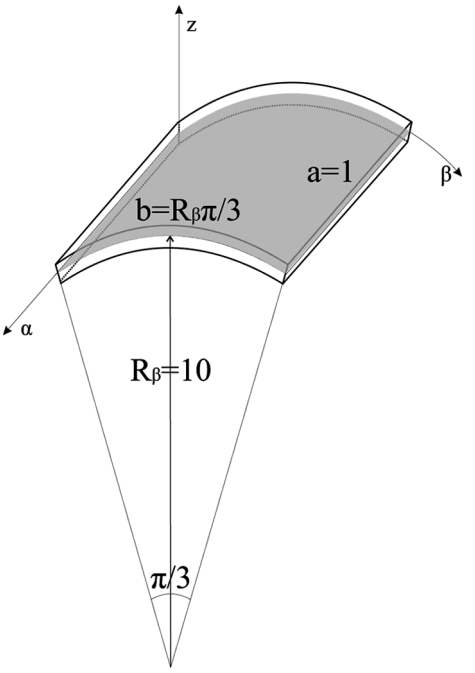

Figure 3 Geometry of Ren shell.

For this two-phase composite material different micromechanical models can be applied for the computation of the effective local material properties. According to [32], the following formulas are chosen:

- The effective bulk modulus B and shear modulus μ are given by the mean field estimate of Mori and Tanaka [33, 34]:

$$\frac{B - B_m}{B_c - B_m} = \frac{V_2}{1 + (1 - V_2)\frac{B_c - B_m}{B_m + \frac{4}{3}\mu_m}} \tag{34}$$

$$\frac{\mu - \mu_m}{\mu_c - \mu_m} = \frac{V_2}{1 + (1 - V_2)\frac{\mu_c - \mu_m}{\mu_m + f_1}} \quad \text{with } f_1 = \frac{\mu_m(9B_m + 8\mu_m)}{6(B_m + 2\mu_m)} \tag{35}$$

- The effective heat conduction coefficient K is given by the model of Hatta and Taya [35]:

$$\frac{K - K_m}{K_c - K_m} = \frac{V_2}{1 + (1 - V_2)\frac{K_c - K_m}{3K_m}} \tag{36}$$

- For the coefficient of thermal expansion α a correspondence relation holds [36, 37], reading:

$$\frac{\alpha - \alpha_m}{\alpha_c - \alpha_m} = \frac{\frac{1}{B} - \frac{1}{B_m}}{\frac{1}{B_c} - \frac{1}{B_m}} \tag{37}$$

In Eqs. (34) to (37), the indices m and c refer to the metallic and ceramic phase, respectively. V_2 is the volume fraction of the ceramic phase that is assumed for the computations as:

$$V_2 = V_c = (z/h)^{n_g} \tag{38}$$

where by changing the exponent n_g different material gradients can be accomplished. Figure 4 shows the through-thickness distribution of the volume fraction V_c of the ceramic phase and the resulting evolution of the bulk modulus.

At the top surface, the shell is subjected to pure mechanical or pure thermal, transverse bi-sinusoidal loads, reading:

$$p_z^+ = \hat{p}_z^+ \sin\left(\frac{m\,\pi\,\alpha}{a}\right) \sin\left(\frac{n\,\pi\,\beta}{b}\right) \quad T^+ = \widehat{T}^+ \sin\left(\frac{m\,\pi\,\alpha}{a}\right) \sin\left(\frac{n\,\pi\,\beta}{b}\right) \tag{39}$$

Here m, n are the wave numbers and a, b the shell dimensions, respectively. A quantity with a superimposed hat denotes the amplitude of the respective load. Since a linear theory is considered, more complicated load cases can be accomplished by superimposing the pure thermal and mechanical contributions.

As an analytical Navier-type solution is employed, the shell is assumed to be simply supported, i.e., the boundary conditions read:

$$\begin{aligned} u_\beta = u_z = 0 \quad &\text{at } \alpha = 0, a \\ u_\alpha = u_z = 0 \quad &\text{at } \beta = 0, b \\ T = 0 \quad &\text{at } \alpha = 0, a \text{ and } \beta = 0, b \end{aligned} \tag{40}$$

which is fulfilled by the assumed harmonic in-plane displacement and temperature fields, compare Eqs. (33). In addition, $m = n = 1$ is assumed for the wave numbers.

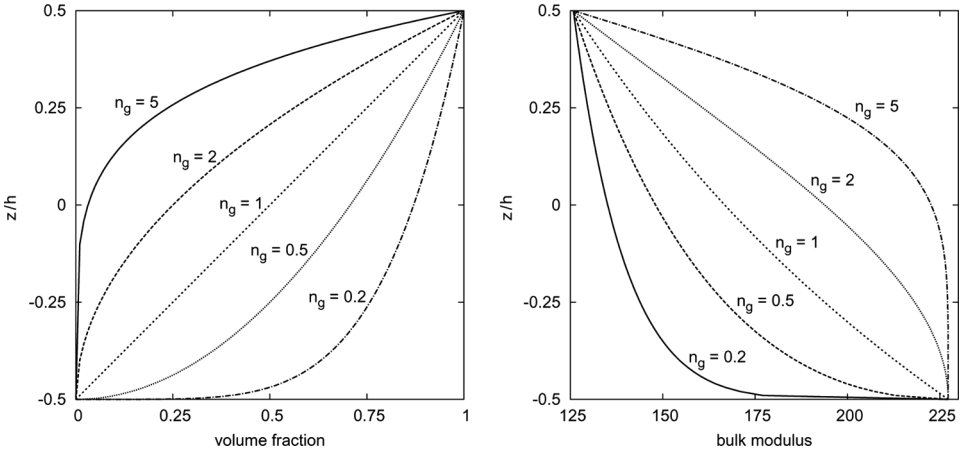

Figure 4 Through-thickness distribution of the volume fraction V_c of the ceramic phase (left) and of the bulk modulus (right).

Table 1 Mechanical load. Non-dimensional transverse displacement $\bar{w}$ and in-plane displacement $\bar{u}$ at the middle (m) of the considered plate ($n_g = 2$). 3D solution is reported in [32]

	$a/h = 4$				$a/h = 10$			
	$3D$	$LD1$	$LD3$	$LD5$	$3D$	$LD1$	$LD3$	$LD5$
$\bar{w}$(m)	−13.70	−10.83	−13.71	−13.70	−170.7	−125.9	−170.7	−170.7
$\bar{u}$(m)	−0.08998	−0.05419	−0.09095	−0.08991	0.7108	0.7807	0.7109	0.7112

As done in [32], non-dimensionalized quantities are introduced:

$$\bar{u}_i = \frac{\hat{u}_i(z)}{P\,a} \quad \bar{\sigma}_{ij} = \frac{\hat{\sigma}_{ij}(z)}{P\,B^*} \quad \overline{T} = \frac{\alpha^* \widehat{T}(z)}{P} \tag{41}$$

where either $P = \hat{p}_z^+/B^*$ or $P = \alpha^* \widehat{T}^+$ is taken for the applied load p_z^+ or for the applied temperature T^+ at the top, respectively. The scale factors are $B^* = 1\,\text{GPa}$ and $\alpha^* = 1 \times 10^6$. The indices i and j can be α, β and z.

Preliminary Assessment

Exact solutions about thermo-mechanical analysis of FGM shells have not been found. To validate the considered shell theories, the quasi-3D solution shown below is considered.

In [26], the results obtained by performing the thermo-mechanical analysis of FGM plates are proposed. In particular, a rectangular plate comprising a single functionally graded layer is considered. Material properties, boundary conditions and loading cases are those seen above for the shell panel. Values of displacement components, obtained by using the theory presented in the previous sections, are resumed in Tables 1 and 2. One can note that fundamental nuclei for the shell are an extension of plate ones. A plate consists of a particular shell with infinite curvature radii R_α and R_β, metric coefficients H_α and H_β are 1 and the matrixes A_p and A_n are zero. In such a case the shell fundamental nuclei degenerate into plate ones.

Quoted results are in very good agreement with the 3D solution reported in [32] for both mechanical (with $N = 6$) and thermal load (with $N = 14$). It is possible to obtain the same values by introducing a number of fictitious "mathematical" layers. That number has been chosen to coincide with the one leading to convergent solutions (a layer-wise theory with an order of expansion equal to 4 has been used in each factious layer).

Table 2 Thermal load. Non-dimensional transverse displacement $\bar{w}$ and in-plane displacement $\bar{u}$ at the middle (m) of the considered plate ($n_g = 2$). 3D solution is reported in [32]

	$a/h = 4$				$a/h = 50$			
	$3D$	$LD1(T_c)$	$LD6(T_c)$	$LD14(T_c)$	$3D$	$LD1(T_c)$	$LD6(T_c)$	$LD14(T_c)$
$\bar{w}$(m)	2.143	4.453	2.170	2.144	28.45	55.52	28.74	28.46
$\bar{u}$(m)	−0.6822	−1.370	−0.6841	−0.6822	−0.8081	−1.348	−0.8101	−0.8080

The above technique is applied in this work to get a reference solution for thermomechanical analysis of the functionally graded shell panel; related results are said quasi-3D solution.

Analysis of the Temperature Profile $T(z)$

Since in the present model the temperature is taken into account as an external loading, its through-thickness distribution must be given a priori as an input to the formulation. In the open literature the temperature field is often assumed to vary linearly between the plate's top and bottom surface values, see e.g., [39]. To compute the actual through-thickness distribution of the temperature for any given material gradient n_g and shell dimensions, the heat-conduction Fourier theory has been used in this work. The boundary conditions at the top and bottom surface of the shell read, respectively:

$$\overline{T}^{+} = 1 \quad \text{at } z = +\frac{h}{2} \quad \overline{T}^{-} = 0 \quad \text{at } z = -\frac{h}{2} \tag{42}$$

Figure 5 depicts the through-thickness distribution of the non-dimensionalized temperature $\overline{T}$ for a shell thickness ratio of $R_\beta/h = 10$, $n_g = 2$ and different orders of expansion N. It can be seen that it is necessary an order of expansion equal to 14 to reach the convergence for temperature. For implementation reasons, the same order of expansion is used to approximate the displacement components but in the following sections it will be shown that in pure-mechanical case a lower value of N is sufficient to obtain the required accuracy. Furthermore, one can note that the temperature distribution is strongly nonlinear which contradicts the assumption of a linear temperature variation often found in the literature. In [26] it is demonstrated that a linear profile can be assumed only for very thin "classical" layers; as far as

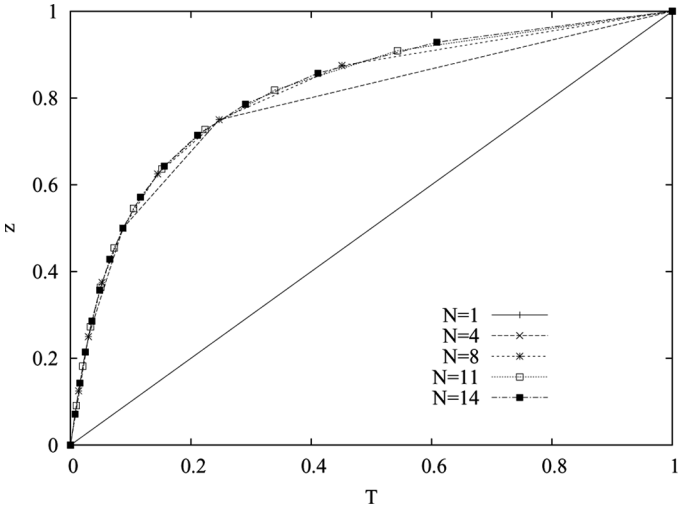

Figure 5 Ren shell ($n_g = 2, R_\beta/h = 10$). Calculated temperature profile T_c.

Table 3 Mechanical load. Non-dimensional transverse displacement $\bar{w}$ and in-plane displacement $\bar{u}$ at top (t), middle (m) and bottom (b) of the considered shell ($n_g = 2$). *Ref* is the solution obtained with $N_{ml} = 100$ mathematical layers

	$R_\beta/h = 10$				$R_\beta/h = 500$			
	Ref	*LD*1	*LD*3	*LD*6	*Ref*	*LD*1	*LD*3	*LD*6
$\bar{w}$(t)	0.0039	0.0032	0.0040	0.0039	2.2199	2.0431	2.2199	2.2199
$\bar{w}$(m)	0.0021	0.0021	0.0022	0.0021	2.2212	2.0437	2.2211	2.2212
$\bar{w}$(b)	0.0013	0.0011	0.0013	0.0013	2.2214	2.0443	2.2214	2.2214
$\bar{u}$(t)	−0.0012	−0.0004	−0.0011	−0.0012	−0.4870	−0.4580	−0.4870	−0.4870
$\bar{u}$(m)	0.0006	0.0003	0.0006	0.0006	0.2099	0.1832	0.2100	0.2100
$\bar{u}$(b)	0.0010	0.0011	0.0010	0.0010	0.9072	0.8244	0.9071	0.9072

the alteration of the temperature distribution due to different material gradients n_g, the influence of the material composition is shown to be considerable.

Transverse Deflection under Thermal and Mechanical Load

In this section, the results obtained by CUF extended to FGM shells under pure thermal or pure mechanical loading are compared with quasi-3*D* solution. Tables 3–6 provide results for the displacement components and in-plane/transverse stresses in non-dimensionalized form for different shell thickness ratios

Table 4 Mechanical load. Non-dimensional stresses $\bar{\sigma}_{ij}$ at top (t), middle (m) and bottom (b) of the considered shell ($n_g = 2$). *Ref* is the solution obtained with $N_{ml} = 100$ mathematical layers

	$R_\beta/h = 10$				$R_\beta/h = 500$			
	Ref	*LD*1	*LD*3	*LD*6	*Ref*	*LD*1	*LD*3	*LD*6
$\bar{\sigma}_{\beta\beta}$(t)	0.6770	0.3703	0.7392	0.6758	441.03	479.99	437.16	440.23
$\bar{\sigma}_{\beta\beta}$(m)	0.1571	0.2135	0.1413	0.1566	381.70	374.26	381.94	381.69
$\bar{\sigma}_{\beta\beta}$(b)	−0.2194	−0.2399	−0.3737	−0.2196	229.93	32.776	235.44	229.89
$\bar{\sigma}_{\alpha z}$(m)	0.4440	0.3303	0.4513	0.4435	6.4016	5.3208	6.4139	6.4017
$\bar{\sigma}_{zz}$(m)	0.4486	0.4602	0.4404	0.4482	0.4494	38.780	0.9361	0.4526

Table 5 Thermal load. Non-dimensional transverse displacement $\bar{w}$ and in-plane displacement $\bar{u}$ at top (t), middle (m) and bottom (b) of the considered shell ($n_g = 2$). *Ref* is the solution obtained with $N_{ml} = 100$ mathematical layers

	$R_\beta/h = 50$				$R_\beta/h = 1000$			
	Ref	*LD*2(T_c)	*LD*8(T_c)	*LD*14(T_c)	*Ref*	*LD*2(T_c)	*LD*8(T_c)	*LD*14(T_c)
$\bar{w}$(t)	7.1337	8.8684	7.1548	7.1361	43.590	48.034	43.653	43.600
$\bar{w}$(m)	6.4131	8.0312	6.4331	6.4153	43.553	47.990	43.617	43.563
$\bar{w}$(b)	6.1942	7.8766	6.2143	6.1964	43.554	47.997	43.618	43.564
$\bar{u}$(t)	−3.5466	−4.1620	−3.5545	−3.5477	−1.7868	−1.8872	−1.7886	−1.7871
$\bar{u}$(m)	−1.4532	−1.5217	−1.4547	−1.4535	−1.1021	−1.1326	−1.1029	−1.1023
$\bar{u}$(b)	0.4833	0.9074	0.4880	0.4837	−0.4178	−0.3785	−0.4176	−0.4178

Table 6 Thermal load. Non-dimensional stresses $\bar{\sigma}_{ij}$ at top (t), middle (m) and bottom (b) of the considered shell ($n_g = 2$). *Ref* is the solution obtained with $N_{ml} = 100$ mathematical layers

	$R_\beta/h = 50$				$R_\beta/h = 1000$			
	Ref	$LD2(T_c)$	$LD8(T_c)$	$LD14(T_c)$	*Ref*	$LD2(T_c)$	$LD8(T_c)$	$LD14(T_c)$
$\bar{\sigma}_{\beta\beta}$(t)	−1481.4	−1409.8	−1470.8	−1470.4	−1170.2	−1098.6	−1159.3	−1159.2
$\bar{\sigma}_{\beta\beta}$(m)	−422.78	−205.82	−419.74	−422.76	159.55	392.59	159.63	159.60
$\bar{\sigma}_{\beta\beta}$(b)	8.4708	−628.63	20.795	7.9878	991.05	554.54	986.16	990.98
$\bar{\sigma}_{\alpha z}$(m)	26.448	−7.3846	26.664	26.459	−5.2242	−6.6837	−5.2415	−5.2262
$\bar{\sigma}_{zz}$(m)	5.0735	319.18	7.5271	5.1982	0.2428	259.60	−1.7681	0.3165

and exponential index $n_g = 2$. It can be concluded that Unified Formulation yields very accurate results compared to quasi-3*D* solution for both mechanical and thermal case and even for very thick shells.

In Figure 6 the through-thickness distribution of the transverse deflection u_z is shown for different material gradients n_g. It can be clearly seen that in the case of thermal loading the transverse deflection varies considerably through the thickness, in respect to the pure-mechanical case, even if the shell is very thin ($R_\beta/h = 100$). This is due to the combined effects of the varying thermal field (see Fig. 5) as well as the altering mechanical properties. Therefore, the usual assumption of a constant through-thickness distribution of u_z made by most lower order shell theories is not justified in the thermal case. However, in the case of a pure mechanical loading, the influence of different material gradients n_g is less pronounced. Furthermore, the variation of the transverse deflection u_z through the thickness is small so in the mechanical case the assumption of a constant through-thickness distribution is valid. Figures 7 and 8 show the through-thickness distribution of the transverse shear and normal stresses, respectively. It can be seen that load boundary conditions are verified for $N = 6$ in the mechanical case and for $N = 14$ in the thermal case.

One can conclude that the use of higher order shell theories is mandatory to capture all the effects of the displacement and stress distributions. By comparing the cases of thermal and mechanical loading, it is shown that a thermal load requires

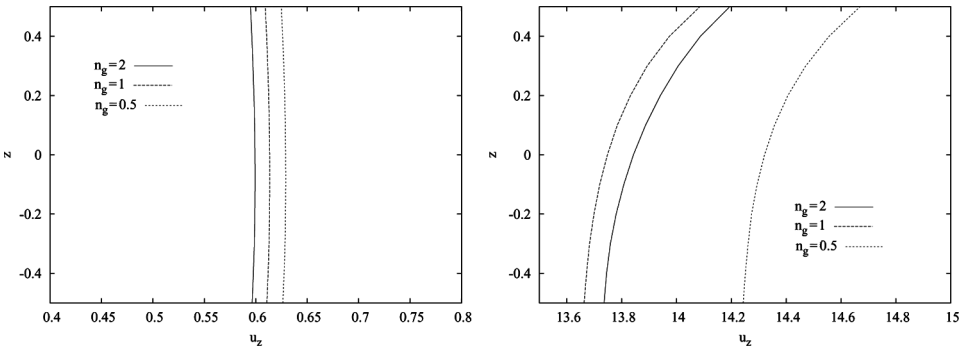

Figure 6 Ren shell ($R_\beta/h = 100$). Transverse displacement u_z: mechanical load [$N = 6$] (left); thermal load [$N = 14$] (right).

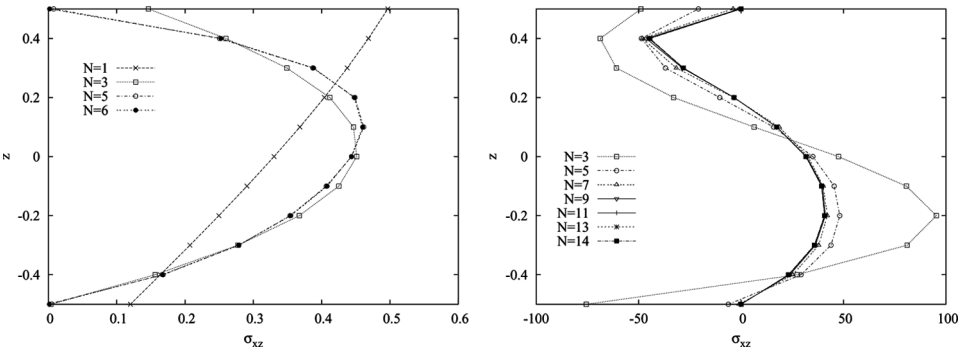

Figure 7 Ren shell ($n_g = 2$, $R_\beta/h = 10$). Transverse shear stress σ_{xz}: mechanical load (left); thermal load (right).

higher order thickness assumptions. As stated in the previous section, this is due to the coupling between the thermal and the mechanical field which claims higher order thickness assumptions to obtain the same accuracy.

CONCLUSIONS

An extension of the Carrera's Unified Formulation which accounts for functionally graded shells subjected to thermal loads has been presented in this work. It has been shown that the unified treatment of all the considered variables (displacements, temperature, material) can include any kind of material gradient. CUF provides very accurate results, compared to reference solutions, although the use of higher order expansions in the thickness direction are mandatory. It has been found that the temperature profile cannot be assumed linear in an FGM layer, even when a very thin shell is considered. The assumption of a constant transverse deflection through the thickness direction is not valid in the thermal case; lower errors are introduced for the mechanical loading. The influence of material gradient is more significant for a thermal loading than for mechanical loadings.

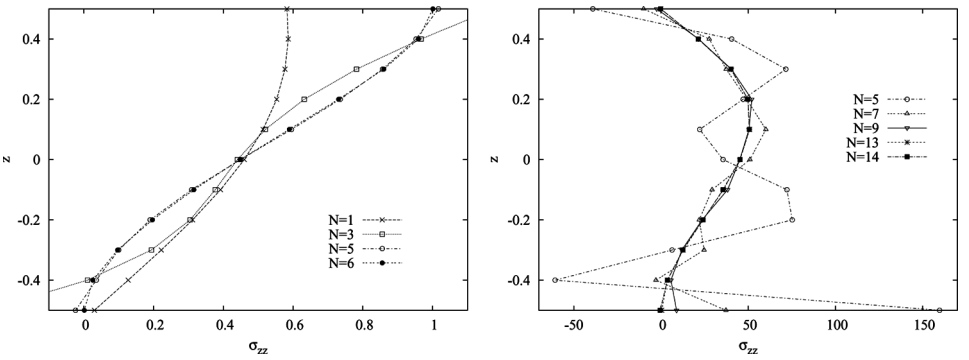

Figure 8 Ren shell ($n_g = 2$, $R_\beta/h = 10$). Transverse normal stress σ_{zz}: mechanical load (left); thermal load (right).

REFERENCES

1. M. Koizumi, The Concept of FGM, *Ceram. Trans. Funct. Graded Mater.*, vol. 34, pp. 3–10, 1993.
2. S. Suresh and A. Mortensen, *Fundamentals of Functionally Graded Materials*, Barnes and Noble Publications, New York, 1998.
3. D. E. Burkes and J. J. Moore, Microstructure and Kinetics of a Functionally Graded NiTi–TiC_x Composite Produced by Combustion Synthesis, *Journal of Alloys and Compounds*, vol. 430, pp. 274–281, 2007.
4. H. Chung and S. Das, Processing and Properties of Glass Bead Particulate-Filled Functionally Graded Nylon-11 Composites Produced by Selective Laser Sintering, *Materials Science and Engineering A*, vol. 437, pp. 226–234, 2006.
5. K. A. Khor, Y. W. Gu, and Z. L. Dong, Mechanical Behavior of Plasma Sprayed Functionally Graded YSZ/NiCoCrAlY Composite Coatings, *Surface and Coatings Technology*, vol. 139, pp. 200–206, 2001.
6. J. I. Kim, W.-J. Kim, D. J. Choi, J. Y. Park, and W.-S. Ryu, Design of a C/SiC Functionally Graded Coating for the Oxidation Protection of C/C Composites, *Carbon A*, vol. 43, pp. 1749–1757, 2005.
7. J. Aboudi, *Mechanics of Composite Materials: A Unified Micromechanical Approach*, Elsevier, New York, 1991.
8. J. Aboudi, M.-J. Pindera, and S. M. Arnold, Higher-Order Theory for Functionally Graded Materials, *Composites Part B: Engineering*, vol. 30, pp. 777–832, 1999.
9. T. Reiter, G. J. Dvorak, and V. Tvergaard, Micromechanical Models for Graded Composite Materials, *Journal of the Mechanics and Physics of Solids*, vol. 45, pp. 1281–1302, 1997.
10. J. R. Zuiker, Functionally Graded Materials: Choice of Micromechanics Model and Limitation in Property Variation, *Composites Engineering*, vol. 5, pp. 807–819, 1995.
11. J. L. Pelletier and S. S. Vel, An Exact Solution for the Steady-State Thermoelastic Response of Functionally Graded Orthotropic Cylindrical Shells, *International Journal of Solids and Structures*, vol. 43, pp. 1131–1158, 2006.
12. Z. S. Shao, Mechanical and Thermal Stresses of a Functionally Graded Circular Hollow Cylinder with Finite Length, *International Journal of Pressure Vessels and Piping*, vol. 82, pp. 155–163, 2005.
13. K. M. Liew, S. Kitipornchai, X. Z. Zhang, and C. W. Lim, Analysis of the Thermal Stress Behaviour of Functionally Graded Hollow Circular Cylinders, *International Journal of Solids and Structures*, vol. 40, pp. 2355–2380, 2003.
14. S. S. Vel and R. Baskiyar, Thermally Induced Stresses in Functionally Graded Thick Tubes, *AIP Conference Proceedings*, vol. 973, pp. 688–693, 2008.
15. K. Abrinia, H. Naee, F. Sadeghi, and F. Djavanroodi, New Analysis for the FGM Thick Cylinders under Combined Pressure and Temperature Loading, *American Journal of Applied Sciences*, vol. 5, no. 7, pp. 852–859, 2008.
16. Z. S. Shao and T. J. Wang, Three-Dimensional Solutions for the Stress Fields in Functionally Graded Cylindrical Panel with Finite Length and Subjected to Thermal/Mechanical Loads, *International Journal of Solids and Structures*, vol. 43, pp. 3856–3874, 2006.
17. C. Chinosi and L. Della Croce, Mixed-Interpolated Finite Elements for Functionally Graded Cylindrical Shells, *Composite Structures*, 2009, accepted.
18. R. Naghdabadi and S. A. Hosseini Kordkheili, A Finite Element Formulation for Analysis of Functionally Graded Plates and Shells, *Archive of Applied Mechanics*, vol. 74, pp. 375–386, 2005.

19. S. A. Hosseini Kordkheili and R. Naghdabadi, Geometrically Non-Linear Thermoelastic Analysis of Functionally Graded Shells using Finite Element Method, *International Journal for Numerical Methods in Engineering*, vol. 72, pp. 964–986, 2007.
20. A. Bahtui and M. R. Eslami, Coupled Thermoelasticity of Functionally Graded Cylindrical Shells, *Mechanics Research Communications*, vol. 34, pp. 1–18, 2007.
21. Z. S. Shao and G. W. Ma, Thermo-Mechanical Stresses in Functionally Graded Circular Hollow Cylinder with Linearly Increasing Boundary Temperature, *Composite Structures*, vol. 83, pp. 259–265, 2008.
22. E. Carrera, A Class of Two Dimensional Theories for Multilayered Plates Analysis, *Atti Accademia delle Scienze di Torino, Mem Sci. Fis.*, vols. 19–20, pp. 49–87, 1995.
23. E. Carrera, S. Brischetto, and A. Robaldo, *Comparison of Various Kinematics for the Analysis of Functionally Graded Materials Plates*, Presented on ACME 2007, Glasgow (U.K.), 2–3 April 2007.
24. E. Carrera, S. Brischetto, and A. Robaldo, A Variable Kinematic Model for the Analysis of Functionally Graded Materials Plates, *AIAA Journal*, vol. 46, pp. 194–203, 2008.
25. S. Brischetto and E. Carrera, *Mixed Theories for the Analysis of Functionally Graded Materials Plates*, presented on AIMETA 2007, Brescia (Italy), 14–17 September 2007.
26. S. Brischetto, R. Leetsch, E. Carrera, T. Wallmersrerger, and B. Kröplin, Thermo-Mechanical Bending of Functionally Graded Plates, *Journal of Thermal Stresses*, vol. 31, no. 3, pp. 286–308, 2008.
27. http://www.polito.it/MUL2.
28. E. Carrera and L. Demasi, Classical and Advanced Multilayered Plate Elements Based upon PVD and RMVT. Part I. Derivation of Finite Element Matrix, *International Journal for Numerical Methods in Engineering*, vol. 55, pp. 191–231, 2002.
29. E. Carrera and L. Demasi, Classical and Advanced Multilayered Plate Elements Based upon PVD and RMVT. Part II. Numerical Implementations, *International Journal for Numerical Methods in Engineering*, vol. 55, pp. 253–291, 2002.
30. E. Carrera and A. Ciuffreda, Closed Form Solution to Assess Multilayered Plates Theories for Various Thermal Stress Problem, *Journal of Thermal Stresses*, vol. 27, pp. 1001–1031, 2004.
31. N. N. Rogacheva, *The Theory of Piezoelectric Shells and Plates*, CRC Press, Boca Raton, Florida, 1994.
32. J. N. Reddy and Z. N. Chen, Three-Dimensional Thermomechanical Deformations of Functionally Graded Rectangular Plates, *European Journal of Mechanics A/Solids*, vol. 20, no. 5, pp. 841–855, 2001.
33. T. Mori and K. Tanaka, Average Stress in Matrix and Average Elastic Energy of Materials with Misfitting Inclusions, *Acta Metallurgica*, vol. 21, pp. 571–574, 1973.
34. Y. Benveniste, A New Approach to the Application of Mori–Tanaka's Theory in Composite Materials, *Mechanics of Materials*, vol. 6, pp. 147–157, 1987.
35. H. Hatta and M. Taya, Effective Thermal Conductivity of a Misoriented Short Fiber Composite, *Journal of Applied Physics*, vol. 58, pp. 2478–2486, 1985.
36. V. M. Levin, Thermal Expansion Coefficients of Heterogeneous Materials, *Mekh. Tverd. Tela*, vol. 2, pp. 88–94, 1967.
37. R. A. Shapery, Thermal Expansion Coefficients of Composite Materials Based on Energy Principles, *Journal of Composite Materials*, vol. 2, pp. 380–404, 1968.
38. S. Brischetto and E. Carrera, Thermal Stress Analysis by Refined Multilayered Composite Shell Theories, *Journal of Thermal Stresses*, vol. 32, nos. 1–2, pp. 165–186, 2009.
39. K. Bhaskar, T. K. Varadan, and J. S. M. Ali, Thermoelastic Solution for Orthotropic and Anisotropic Composites Laminates, *Composites Part B*, vol. 27, pp. 415–420, 1996.

APPENDIX A

The explicit expressions of the fundamental nuclei are listed below for the case of a closed form solution. $\alpha = m\pi/a$ and $\beta = n\pi/b$, with m, n as the wave numbers in in-plane directions and a, b as the shell dimensions.

Introducing the following notations:

$$\left(J^{k\tau sr}, J^{k\tau sr}_{\alpha}, J^{k\tau sr}_{\beta}, J^{k\tau sr}_{\frac{\alpha}{\beta}}, J^{k\tau sr}_{\frac{\beta}{\alpha}}, J^{k\tau sr}_{\alpha\beta}\right) = \int_{A_k} F_r F_\tau F_s \left(1, H^k_\alpha, H^k_\beta, \frac{H^k_\alpha}{H^k_\beta}, \frac{H^k_\beta}{H^k_\alpha}, H^k_\alpha H^k_\beta\right) dz$$

$$\left(J^{k\tau_z sr}, J^{k\tau_z sr}_{\alpha}, J^{k\tau_z sr}_{\beta}, J^{k\tau_z sr}_{\frac{\alpha}{\beta}}, J^{k\tau_z sr}_{\frac{\beta}{\alpha}}, J^{k\tau_z sr}_{\alpha\beta}\right) = \int_{A_k} F_r \frac{\partial F_\tau}{\partial z} F_s \left(1, H^k_\alpha, H^k_\beta, \frac{H^k_\alpha}{H^k_\beta}, \frac{H^k_\beta}{H^k_\alpha}, H^k_\alpha H^k_\beta\right) dz$$

$$\left(J^{k\tau s_z r}, J^{k\tau s_z r}_{\alpha}, J^{k\tau s_z r}_{\beta}, J^{k\tau s_z r}_{\frac{\alpha}{\beta}}, J^{k\tau s_z r}_{\frac{\beta}{\alpha}}, J^{k\tau s_z r}_{\alpha\beta}\right) = \int_{A_k} F_r F_\tau \frac{\partial F_s}{\partial z} \left(1, H^k_\alpha, H^k_\beta, \frac{H^k_\alpha}{H^k_\beta}, \frac{H^k_\beta}{H^k_\alpha}, H^k_\alpha H^k_\beta\right) dz$$

$$\left(J^{k\tau_z s_z r}, J^{k\tau_z s_z r}_{\alpha}, J^{k\tau_z s_z r}_{\beta}, J^{k\tau_z s_z r}_{\frac{\alpha}{\beta}}, J^{k\tau_z s_z r}_{\frac{\beta}{\alpha}}, J^{k\tau_z s_z r}_{\alpha\beta}\right) = \int_{A_k} F_r \frac{\partial F_\tau}{\partial z} \frac{\partial F_s}{\partial z} \left(1, H^k_\alpha, H^k_\beta, \frac{H^k_\alpha}{H^k_\beta}, \frac{H^k_\beta}{H^k_\alpha}, H^k_\alpha H^k_\beta\right) dz$$

where z indicates the partial derivative with respect to z, fundamental nuclei K_{uu} and $K_{u\theta}$ can be written in compact form as:

- K_{uu}

$$K_{uu_{11}} = C^k_{55} J^{k\tau_z s_z r}_{\alpha\beta} + \frac{1}{R^k_\alpha} C^k_{55}\left(-J^{k\tau_z sr}_{\beta} - J^{k\tau s_z r}_{\beta} + \frac{1}{R^k_\alpha} J^{k\tau sr}_{\beta/\alpha}\right) + C^k_{11} J^{k\tau sr}_{\beta/\alpha}\alpha^2 + C^k_{66} J^{k\tau sr}_{\alpha/\beta}\beta^2$$

$$K_{uu_{12}} = J^{k\tau sr}\alpha\beta(C^k_{12} + C^k_{66}) = K_{uu_{21}}$$

$$K_{uu_{13}} = C^k_{55}\left(J^{k\tau_z sr}_{\beta}\alpha - \frac{1}{R^k_\alpha} J^{k\tau sr}_{\beta/\alpha}\alpha\right) - C^k_{13} J^{k\tau s_z r}_{\beta}\alpha - \frac{1}{R^k_\alpha} C^k_{11} J^{k\tau sr}_{\beta/\alpha}\alpha - C^k_{12} J^{k\tau sr}\alpha\frac{1}{R^k_\beta}$$

$$K_{uu_{22}} = C^k_{44} J^{k\tau_z s_z r}_{\alpha\beta} + \frac{1}{R^k_\beta} C^k_{44}\left(-J^{k\tau_z sr}_{\alpha} - J^{k\tau s_z r}_{\alpha} + \frac{1}{R^k_\beta} J^{k\tau sr}_{\alpha/\beta}\right) + C^k_{22} J^{k\tau sr}_{\alpha/\beta}\beta^2 + C^k_{66} J^{k\tau sr}_{\beta/\alpha}\alpha^2$$

$$K_{uu_{23}} = C^k_{44}\left(J^{k\tau_z sr}_{\alpha}\beta - \frac{1}{R^k_\beta} J^{k\tau sr}_{\alpha/\beta}\beta\right) - C^k_{23} J^{k\tau s_z r}_{\alpha}\beta - \frac{1}{R^k_\beta} C^k_{22} J^{k\tau sr}_{\alpha/\beta}\beta - \frac{1}{R^k_\alpha} C^k_{12} J^{k\tau sr}\beta$$

$$K_{uu_{31}} = C^k_{55} J^{k\tau s_z r}_{\beta}\alpha - C^k_{55}\frac{1}{R^k_\alpha} J^{k\tau sr}_{\beta/\alpha}\alpha - C^k_{13} J^{k\tau_z sr}_{\beta}\alpha - \frac{1}{R^k_\alpha} C^k_{11} J^{k\tau sr}_{\beta/\alpha}\alpha - \frac{1}{R^k_\beta} C^k_{12} J^{k\tau sr}\alpha$$

$$K_{uu_{32}} = C^k_{44}\left(J^{k\tau s_z r}_{\alpha}\beta - \frac{1}{R^k_\beta} J^{k\tau sr}_{\alpha/\beta}\beta\right) - C^k_{23} J^{k\tau_z sr}_{\alpha}\beta - \frac{1}{R^k_\beta} C^k_{22} J^{k\tau sr}_{\alpha/\beta}\beta - \frac{1}{R^k_\alpha} C^k_{12} J^{k\tau sr}\beta$$

$$K_{uu_{33}} = C_{55}^k J_{\beta/\alpha}^{k\tau sr}\alpha^2 + C_{44}^k J_{\alpha/\beta}^{k\tau sr}\beta^2 + C_{33}^k J_{\alpha\beta}^{k\tau_z s_z r} + \frac{1}{R_\alpha^k}\left(\frac{1}{R_\alpha^k}C_{11}^k J_{\beta/\alpha}^{k\tau sr} + C_{13}^k J_\beta^{k\tau s_z r} + C_{13}^k J_\beta^{k\tau_z sr}\right)$$
$$+ \frac{2}{R_\alpha^k R_\beta^k} J^{k\tau sr} C_{12}^k + \frac{1}{R_\beta^k}\left(\frac{1}{R_\beta^k}C_{22}^k J_{\alpha/\beta}^{k\tau sr} + C_{23}^k J_\alpha^{k\tau_z sr} + C_{23}^k J_\alpha^{k\tau s_z r}\right)$$

- $K_{u\theta}$

$$K_{u\theta_1} = \alpha J_\beta^{k\tau sr}\lambda_{p1}^k$$
$$K_{u\theta_2} = \beta J_\alpha^{k\tau sr}\lambda_{p2}^k$$
$$K_{u\theta_3} = -J_\beta^{k\tau sr}\frac{1}{R_\alpha^k}\lambda_{p1}^k - J_\alpha^{k\tau sr}\frac{1}{R_\beta^k}\lambda_{p2}^k - J_{\alpha\beta}^{k\tau_z sr}\lambda_{n3}^k$$